

# Characterizing the formation and growth of intermetallic compound in the solder joint

Y. G. LEE, J. G. DUH\*

Department of Materials and Engineering, National Tsing Hua University, Hsinchu, Taiwan  
E-mail: ydxu@nwp.edu.cn

A solder/intermetallic layers/copper joint assembly was prepared by the dipping process and then aged thermally for an accelerating aging test. The phase transformation of the assembly was compared to the phase diagram of binary alloy, Cu–Sn, and it showed an agreement with the resultant intermetallic phases formed between the pure tin and pure copper. Two theoretical models proposed by Gösele and Shatynski were developed and then employed to characterize the assembly. The Gösele's model was used to predict whether the intermetallic layers grew or shrank during aging, while the Shatynski's model was employed to estimate the related reactive thicknesses and hence the ratios of the interdiffusivities in the joint assembly. After a series of calculations, the Gösele's model predicted that  $\text{Cu}_6\text{Sn}_5$  and  $\text{Cu}_3\text{Sn}$  intermetallic layers became thicker; the orders of the intermetallic interdiffusivities were also proven to approach theoretical values from the Shatynski's model. © 1998 Kluwer Academic Publishers

## 1. Introduction

To meet the critical trends of miniaturization, lighter weight, and multi-function in today's electronic industry, modern packaging technology has advanced to the point of achieving maximum density. Solder joints serving as mechanical support and heat dissipater are especially designed not only to be reliable when subjected to hostile environments but also to be cost effective [1]. To meet these requirements, for the former, unleaded solder is one of the best candidates to replace the traditional Pb–Sn solder, [2–5] and for the latter, copper could substitute for the noble-metal-containing metallization [6]. To adhere to the conductor, intermetallic compound (IMC) has to form and serve as the surface activator between the solder and metallization. However, IMC occasionally poses a weakness in the solder joint and causes microstrains due to the mismatch of thermal expansion coefficient (CTE) between the solder and IMC. As the microstrains exceed a critical value, microcracks occur at the interface of solder/IMC and might propagate, which would result in failure of the joint and hence influence the solder joint's reliability. It is argued that the degradation of the solder joint is related to the IMC thickness and to the kinetics of IMC growth during aging [7]. With the increasing IMC thickness, different fracture modes and delimitation positions take place in the joint and consequently degrade the solder joint's reliability. Much research has been focused on the mechanism of IMC formation during soldering and on its growth kinetics during the aging process [8–11]. Preliminary studies on the formation and growth of IMC in an unleaded solder joint were investigated by our group [12, 13]. Recently, experimen-

tal works on the evaluation of the microstructure and the concentration profile near the interfaces of solder joints has been carried out [14, 15]. The purpose of this research is to predict the formation and growth of IMC in a Sn-containing solder/IMC/Cu joint assembly by the employment and modification of theoretical models. Experimental data will be compared to the theoretical derivation through a series of reaction constants related to the Cu–Sn compound in the consideration of thermodynamics and diffusional fluxes.

## 2. Experimental procedures

A commercial lead-free solder (J.W Harris Co., Cincinnati, OH, USA) was used as the soldering material, and the compositions were Sn:  $98.67 \pm 0.16$  mol %; Cu:  $1.2 \pm 0.05$  mol %; Al:  $0.18 \pm 0.01$  mol %; and Ni  $< 0.02$  mol %, as measured with an electron probe analyzer (EPMA, Jeol, JMA 8800M, Japan). An assembly of solder/IMCs/Cu was designed to simulate the lamination of passive device/IMCs/metallization in this study. A copper substrate was cut into blocks having dimensions of  $6 \text{ mm} \times 6 \text{ mm} \times 0.5 \text{ mm}$ , which were then polished and cleaned ultrasonically in a batch containing acetone and deionized water successively.

The solder was melted at a working temperature of  $268^\circ\text{C}$ , about  $40^\circ\text{C}$  higher than its melting point. The copper blocks were dipped perpendicularly to the surface of the melted solder bath for 3 s and then pulled out perpendicularly, which was followed by air-cooling. The lead-free solder/copper assemblies were dwelled in an aging oven at  $150^\circ\text{C}$ . After aging, the morphologies of the joints were investigated with a scanning electron

\* Author to whom correspondence would be associated.

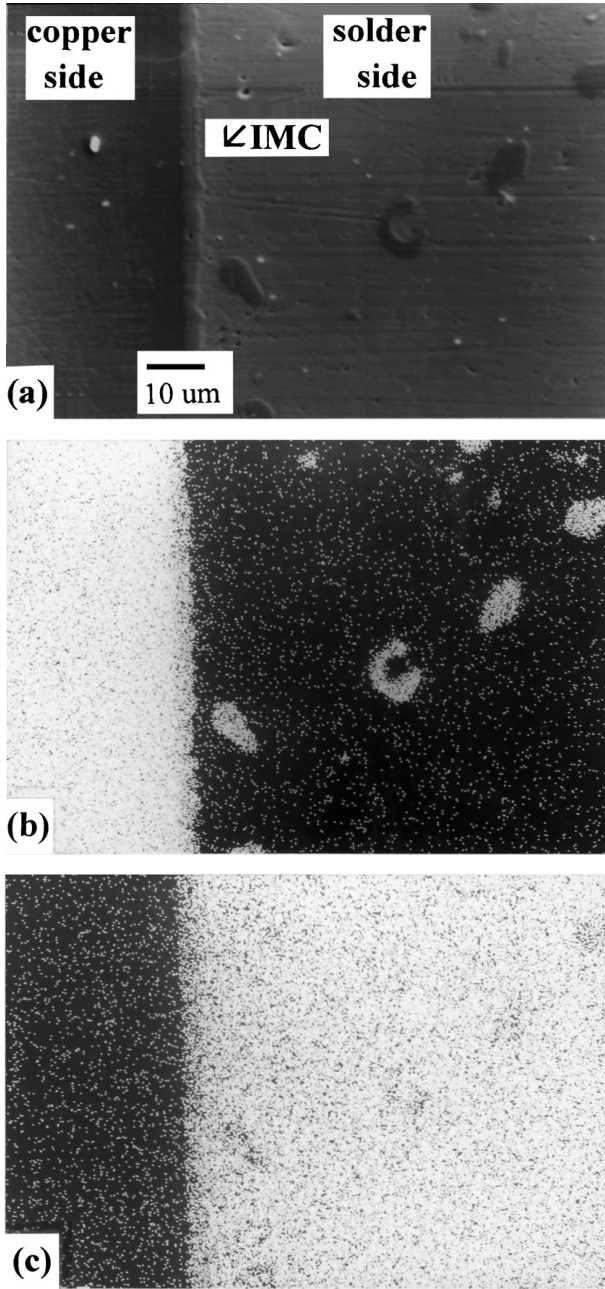


Figure 1 Morphology of the solder/IMCs/copper assembly: (a) SEM; (b) X-ray mapping of copper; and (c) X-ray mapping of tin.

microscope (SEM). An optical microscope (OM) and EPMA were employed to evaluate the thickness and concentration of IMC, respectively.

### 3. Results and discussion

The microstructure of the solder/IMCs/copper assembly and the related mechanism of mass transport were studied with the morphology of the cross-sectional view, as shown in the secondary electron images (SEIs) of Fig. 1a–c.

The intermetallic layers formed between solder and copper, and some precipitates appeared near the interface of the IMCs/solder. The intermetallic layers were identified with an X-ray diffractometer (XRD), and the phases were  $\varepsilon$  ( $\text{Cu}_3\text{Sn}$ ) and  $\eta$  ( $\text{Cu}_6\text{Sn}_5$ ) phases. The compositions of the IMC layer as measured by EPMA were close to  $\text{Cu}_6\text{Sn}_5$  for the layer near the sol-

der side, while they were close to  $\text{Cu}_3\text{Sn}$ , which was near the copper side. With the increasing aging time, the IMC layers thickened, and the local irregularities gradually smoothed. After a series of thickness measurement with OM, the expression of IMC thickness versus the square root of aging time shows a linear dependence as follows

$$\Delta y_i(t) = k_i t^{1/2} \quad (1)$$

where  $\Delta y_i$  is the growth thickness of IMC during aging;  $k_i$  is the coefficient standing for the square root of the diffusivity at the aging temperature; and  $t$  is the aging time. The exponent value, 1/2, in Equation 1 reveals a diffusion-controlled mechanism during aging, and the mass transport for the assembly can be described as a one-dimension diffusional lamination [16].

Recently, an IMC growth theory predicting whether the intermetallic layer grows or shrinks was developed by Gösele [17]. He assumed that the two intermetallic layers are already present with given thicknesses to avoid the complicated introduction about nucleation barrier near a phase boundary. He also introduced a “kinetic instability,” induced by interfacial reaction barriers to determine whether one of the intermetallic layers will grow or shrink under various compositional conditions. In this sense, the IMCs thicknesses are the resulting thicknesses in which the matrix and IMC layers extend to each other, and whether the IMCs grow or shrink depends on the extending thicknesses moving outward toward the two boundaries of the IMC layers. If the net thickness is smaller than zero, i.e., the gaining thickness from one neighboring layer is less than the lost thickness in another neighboring layer, the total IMC thickness shrinks, and vice versa.

By using the Gösele model, the flux ratio  $r$  of  $\varepsilon$  to  $\eta$  is expressed as

$$r = \frac{J_\varepsilon}{J_\eta} = \frac{D_\varepsilon \frac{\partial C_\varepsilon}{\partial x}}{D_\eta \frac{\partial C_\eta}{\partial x}} \quad (2)$$

where  $J_\varepsilon$  and  $J_\eta$ , indicate fluxes of the copper substrate;  $D_\varepsilon$  and  $D_\eta$  are diffusivities of the copper;  $C_\varepsilon$  and  $C_\eta$  represent concentrations in the  $\varepsilon$  phase and  $\eta$  phase; and  $x$  is the distance from the copper side to the solder side. The parameter,  $r$ , is compared to other parameters,  $r_1$  and  $r_2$ , to judge the IMCs’ growth or shrinkage. These two parameters are expressed as

$$r_1 = \frac{(1 + N_{Cu,\eta})(N_{Cu,\alpha} - N_{Cu,\varepsilon})}{(1 + N_{Cu,\varepsilon})(N_{Cu,\alpha} - N_{Cu,\eta})} \quad (3)$$

and

$$r_2 = \frac{(1 + N_{Cu,\eta})(N_{Cu,\varepsilon} - N_{Cu,\beta})}{(1 + N_{Cu,\varepsilon})(N_{Cu,\eta} - N_{Cu,\beta})} \quad (4)$$

where  $N$  is the molar fraction of the copper in the matrix or IMC layer. For the special case in this study, the concentration gradient is assumed to be constant due

to the narrow miscibility in the  $\varepsilon$  and  $\eta$  phases. In addition, the IMC growth thicknesses, illustrated in the next section, are proportional to the square root of the product of intrinsic diffusivity multiplying aging time. Consequently, Equation 2 is simplified to be

$$r = \frac{\Delta C_\varepsilon}{\Delta C_\eta} \frac{\sqrt{D_\varepsilon}}{\sqrt{D_\eta}} \quad (5)$$

where  $\Delta C_\varepsilon$  and  $\Delta C_\eta$  are the miscibility gaps in the intermetallic compound,  $\text{Cu}_3\text{Sn}$  and  $\text{Cu}_6\text{Sn}_5$ , respectively. The resultant flux ratio  $r$  is 0.67, which lies in the range of  $r_1(= 0.46)$  to  $r_2(= 1.93)$ . Under such conditions, both IMC layers are confirmed to grow simultaneously, and the trend of IMC growth observed in this study is in agreement with the model's prediction.

Shatynski *et al.* [18] once derived an expression for the relative number of moles produced in two compound phases. A quantitative prediction was given for the growth or consumption of each product phase with a diffusion-controlled mechanism at the interfaces. Two assumptions were made in the model: There is negligible terminal solid solubility of the reactants, and a quasi-steady-state occurs at the interfaces of the laminated assembly. The so-called "quasi-steady-state growth" is defined in Jost's hypothesis that (1) at the boundaries of a given product phase, the flux of Cu and Sn atoms (for constant cross-section) are inverse functions of the thickness of the phase and that (2) the equilibrium boundary conditions are maintained at interphase interfaces [19]. The schematic plot associated with the assumptions is shown in Fig. 2. To match the calculation of the related parameters in Shatynski's model, two-edge layers representing the terminal solid solutions,  $\text{Cu}_\beta\text{Sn}$  and  $\text{Cu}_\alpha\text{Sn}$ , identified by XRD to be  $\beta$  and  $\alpha$  phases, were  $\text{Cu}_{0.0004}\text{Sn}$  and  $\text{Cu}_{27.57}\text{Sn}$ , respectively. In the same way, IMCs,  $\text{Cu}_\eta\text{Sn}$  ( $\eta$  phase) and  $\text{Cu}_\varepsilon\text{Sn}$

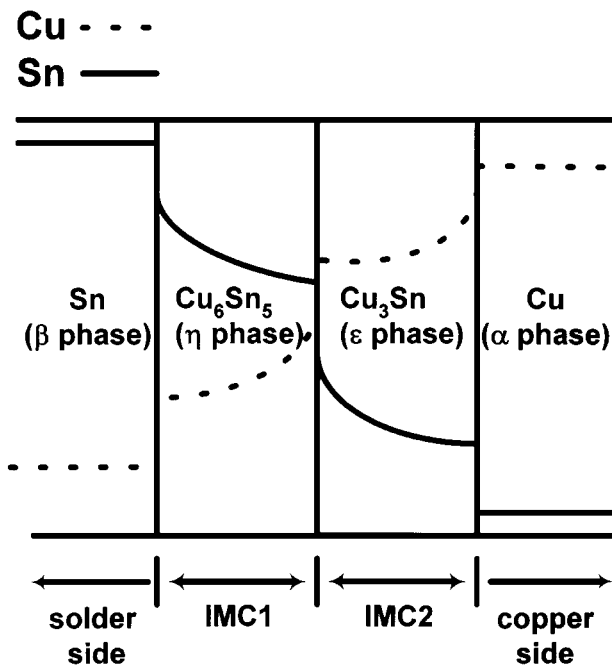
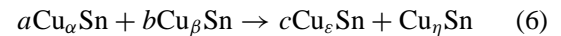


Figure 2 Schematic plot of the concentration profiles for the solder/IMCs/copper assembly.

( $\varepsilon$  phase), formed between these two terminal solution were also re-formulated as  $\text{Cu}_{1.2}\text{Sn}$  and  $\text{Cu}_3\text{Sn}$ , respectively.

In this study the total reaction is represented as



where  $a$ ,  $b$ , and  $c$  are the stoichiometric coefficients in the formula. Mass balance of copper and tin in Equation 6 gives  $a = 0.04 + 0.11c$  and  $b = 0.96 + 0.89c$ . The IMC growth or consumption for the assembly related to the molar volume of the assembly laminate and also to the stoichiometric coefficients is expressed as

$$\frac{X_\eta}{\Omega_\eta} = \frac{X_\varepsilon}{\Omega_\varepsilon}c = \frac{X_\alpha}{\Omega_\alpha}a = \frac{X_\beta}{\Omega_\beta}b \quad (7)$$

where  $\Omega$  is the molar volume;  $X$ , the reaction thickness of the assembly solder/IMCs/Cu; and subscripts  $\eta$ ,  $\varepsilon$ ,  $\alpha$ , and  $\beta$  are the phases. Note that the partitioning factor, ratio of moles of  $\text{Cu}_3\text{Sn}$  to those of  $\text{Cu}_6\text{Sn}_5$  formed after steady-state diffusion, is calculated from a quadratic root of an equation. The partitioning factor is expressed as the following equation

$$c = \frac{e + \sqrt{e^2 + 4fg}}{2g} \quad (8a)$$

where

$$e = \left( \frac{\Omega_\varepsilon}{\Omega_\eta} \right)^2 \left[ \frac{1}{\varepsilon - \eta} h_{\text{Cu}}^\eta + \frac{\eta}{\varepsilon - \eta} h_{\text{Sn}}^\eta \right] - \left[ \frac{1}{\varepsilon - \eta} h_{\text{Cu}}^\varepsilon + \frac{\varepsilon}{\varepsilon - \eta} h_{\text{Sn}}^\varepsilon \right] \quad (8b)$$

$$f = \left( \frac{\Omega_\varepsilon}{\Omega_\eta} \right)^2 \left[ \left( \frac{1}{\varepsilon - \eta} + \frac{1}{\eta - \beta} \right) h_{\text{Cu}}^\eta + \left( \frac{\varepsilon}{\varepsilon - \eta} + \frac{\beta}{\eta - \beta} \right) h_{\text{Sn}}^\eta \right] \quad (8c)$$

and

$$g = \left( \frac{1}{\alpha - \varepsilon} + \frac{1}{\varepsilon - \eta} \right) h_{\text{Cu}}^\varepsilon + \left( \frac{\alpha}{\alpha - \varepsilon} + \frac{\eta}{\varepsilon - \eta} \right) h_{\text{Sn}}^\varepsilon \quad (8d)$$

and the two parameters in Equations 8b-d were expressed as

$$h_{\text{Cu}}^\eta = -\Omega_\eta \int_{C_{\eta\beta}}^{C_{\eta\varepsilon}} D_{\text{Cu}}^\eta dC_{\text{Cu}}^\eta \quad (9a)$$

and

$$h_{\text{Cu}}^\varepsilon = -\Omega_\varepsilon \int_{C_{\varepsilon\eta}}^{C_{\varepsilon\alpha}} D_{\text{Cu}}^\varepsilon dC_{\text{Cu}}^\varepsilon \quad (9b)$$

It is generally assumed that  $D_{\text{Cu}}^{\eta}$  and  $D_{\text{Cu}}^{\varepsilon}$  in this study are not strongly concentration-dependent, thus the parameter  $h_{\text{Cu}}^{\eta}$  and  $h_{\text{Cu}}^{\varepsilon}$  could be simplified to be

$$h_{\text{Cu}}^{\eta} \approx -\Omega_{\eta} D_{\text{Cu}}^{\eta} (C_{\eta\beta} - C_{\eta\varepsilon}) \quad (10a)$$

and

$$h_{\text{Cu}}^{\varepsilon} \approx -\Omega_{\varepsilon} D_{\text{Cu}}^{\varepsilon} (C_{\varepsilon\alpha} - C_{\varepsilon\eta}) \quad (10b)$$

The related parameters  $\Omega_{\varepsilon}$  and  $\Omega_{\eta}$  in Equation 7 are 9.43 and  $10.7 \text{ cm}^3/\text{mole}$ , respectively, from the literature [20]. After a series of substitutions, the value of partitioning factor is calculated to be 3.59. The growth thickness of the IMCs,  $\text{Cu}_3\text{Sn}$  and  $\text{Cu}_6\text{Sn}_5$ , relating to the consumption thickness of the matrix, solder, and copper is calculated by employing Equation 7. This constructs a relationship of mass conservation

$$X_{\alpha} = \frac{X_{\varepsilon}}{0.16} = \frac{X_{\eta}}{0.65} = \frac{X_{\beta}}{0.24} \quad (11)$$

This relationship indicates that the IMCs  $\text{Cu}_3\text{Sn}$  and  $\text{Cu}_6\text{Sn}_5$  grow with a rate 0.16 times and 0.65 times, respectively, that of copper. Furthermore, tin layer has to transport 0.24 times that of the copper layer thickness to serve as the mass source of IMCs. However, if the growth thickness is checked by this relation, the calculated diffusivity ratio of  $\eta$  phase to  $\varepsilon$  phase,  $D_{\eta}/D_{\varepsilon}$ , is 16.06. With respect to the experimental diffusivities of  $D_{\eta}$  and  $D_{\varepsilon}$  at  $2.79 \times 10^{-13}$  and  $6.49 \times 10^{-14} \text{ cm}^2/\text{sec}$ , respectively, it appears that the calculated diffusivity ratio shows a value around four times higher than the experimental diffusivity ratio of 4.34. In fact, according to the relationship  $2k_p^i t = X_i^2$  where  $k_p^i$  is related to interdiffusivity of magnitude, the experimental diffusivity of IMCs can be considered to be ranged over the same order of magnitude as the calculated one.

#### 4. Conclusion

1. The development of the interfacial phase transformation was investigated through the morphology of the solder/ $\text{Cu}_6\text{Sn}_5/\text{Cu}_3\text{Sn}/\text{Cu}$  joint assembly. The thicknesses of the IMC layers grew with a linear dependence of thicknesses versus square root of aging time.

2. Gösele's model was adapted, and it was demonstrated that both IMC layers including  $\text{Cu}_6\text{Sn}_5$  and  $\text{Cu}_3\text{Sn}$  grew and thickened during the aging process. In addition, to compare with Shatynski's derivation,

empirical data in this study were substituted for related parameters in the model, and estimated diffusional ratios for the IMC growth were obtained.

3. This study presents an effective approach to characterize the formation and growth of IMC in the solder joint and further provides a potentially powerful tool in the evaluation of solder joint reliability in the micro-electronic package.

#### Acknowledgement

The authors acknowledge financial support from the National Science Council, Taiwan, under Contracts NSC 86-2221-E-007-043 and NSC 87-2218-E-007-024.

#### References

1. J. GLAZER, *J. Electron. Mater.* **23** (1994) 693.
2. T. A. POWERS, *ibid.* **23** (1994) 773.
3. S. K. KANG, *ibid.* **23** (1994) 701.
4. M. McCORMACK and S. JIN, *ibid.* **23** (1994) 635.
5. *Idem*, *ibid.* **23** (1994) 687.
6. P. T. VIANCO, A. C. KILGO and R. GRANT, *ibid.* **24** (1995) 1493.
7. D. YAO and J. K. SHANG, *Metall. Mater. Trans. A* **26A** (1995) 2677.
8. H. K. KIM and K. N. TU, *Phys. Rev. B* **53** (1996) 160274.
9. K. N. TU and R. D. THOMPSON, *Acta Metall.* **30** (1982) 947.
10. P. T. VIANCO, K. L. ERICKSON and P. L. HOPKINS, *J. Electron. Mater.* **23** (1994) 721.
11. K. L. ERICKSON, P. L. HOPKINS and P. T. VIANCO, *ibid.* **23** (1994) 721.
12. C. C. YOUNG, MS. Dissertation, National Tsing Hua University, Taiwan, Republic of China (1996).
13. J. G. DUH, C. C. YOUNG and Y. G. LEE, in "Proceedings of the Second International Symposium on Electronic Packaging Technology" (Commercial Press Shanghai Plant, Shanghai, China, 1996) p. 330.
14. Y. G. LEE and J. G. DUH, in "1998 Proceedings Pan Pacific Microelectronics Symposium," Kona, Hawaii (Surface Mount Technology Association, Edina, Minnesota, USA) p. 501.
15. Y. G. LEE and J. G. DUH, *J. Mater. Sci in Electron.*, submitted.
16. P. T. VIANCO, P. F. HLAVA and A. C. KILGO, *J. Electron. Mater.* **23** (1994) 583.
17. U. GÖSELE and K. N. TU, *J. Appl. Phys.* **53** (1982) 3252.
18. S. R. SHATYNSKI, J. P. HIRTH and R. A. RAPP, *Acta Metall.* **24** (1976) 1071.
19. W. JOST, in "Diffusion in Solids, Liquids, Gases" 3rd Ed. (Academic Press, New York, 1960) p. 71.
20. M. G. PECHT, in "Soldering Processes and Equipment" (John Wiley & Sons, Inc., New York, USA, 1993) Chap. 1.

Received 1 June

and accepted 14 August 1998